Int. J. Heat Mass Transfer. Vol. 32, No. 10, pp. 1809–1820, 1989
Printed in Great Britain

0017-9310/89 $3.00+0.00

Rayleigh limit–Penndorf extension

AHMET SELAMET and VEDAT S. ARPACI
Department of Mechanical Engineering and Applied Mechanics, University of Michigan, Ann Arbor, MI 48109, U.S.A.

(*Received* 20 *October* 1988 *and in final form* 17 *January* 1989)

Abstract—The Rayleigh limit of the Lorenz–Mie theory is extended by the Penndorf correction. For the efficiency factors, this extension leads to

$$Q^{\mathrm{P}}_{\mathrm{a,s,e}} = Q^{\mathrm{R}}_{\mathrm{a,s,e}}(1+\Pi_{\mathrm{a,s,e}})$$

where superscripts P and R denote Penndorf and Rayleigh; subscripts s, a, and e, respectively, scattering absorption, and extinction; and Π the Penndorf correction to the Rayleigh limit. This correction is shown to extend the Rayleigh limit from $\alpha \cong 0.3$ to 0.8, α being the particle size parameter. Error contours are generated for the Rayleigh and Penndorf limits for $\alpha = 0.3$, 0.5, and 0.7 in the $1.5 \leqslant n \leqslant 2.5$ and $0.5 \leqslant k \leqslant 1.5$ domain which covers the range of soot properties. The practical significance of the Penndorf correction is demonstrated in terms of optical diagnostics and radiative heat transfer. Also, the Planck and Rosseland mean absorption coefficients based on the Penndorf expansion are shown to yield relative to those based on the Rayleigh limit

$$\kappa^{\mathrm{P}}_{\mathrm{P,R}}/\kappa^{\mathrm{R}}_{\mathrm{P,R}} = 1+\Pi^{\mathrm{P}}_{\mathrm{P,R}}(\underbrace{M_1,\ldots,N_1,\ldots,}_{\text{EM waves}}\ \underbrace{\pi DT/C_2}_{\text{Quanta}})$$

where subscripts P and R denote the Planck and Rosseland mean absorption coefficients, superscripts P and R denote Penndorf and Rayleigh, Π the Penndorf correction depending on Ms and Ns which are the explicit functions of refractive and absorptive indices of particles, and on the dimensionless number $\pi DT/C_2$ (D being the particle diameter, T the temperature, and C_2 the second radiation constant). For larger particles and/or higher temperatures the Penndorf based Planck mean coefficient is shown to deviate considerably from the Rayleigh based Planck mean coefficient. This deviation is exhibited to a somewhat lesser extent by the Penndorf based Rosseland mean coefficient.

1. INTRODUCTION

THERMAL radiation from particulate laden media often plays an appreciable role in industrial combustion applications as well as in atmospherical and extraterrestrial problems. Examples are fluidized beds, oil- and gas-fired furnaces, radiative burners, solid propellant rockets, gas turbine combustors, internal combustion engines, natural fires, clouds, fog, atmospheric and interstellar dust. The radiation in these applications depends on the spectral (volume or mass) coefficients which can be obtained from the classical Lorenz–Mie (LM) theory for isotropic, homogeneous spherical particles (see, for example, van de Hulst [1], Kerker [2], Deirmendjian [3], Born and Wolf [4], Jones [5], Bayvel and Jones [6], and Bohren and Huffman [7]). The Rayleigh approximation to the LM theory is widely utilized when the particle diameter is small relative to the wavelength of radiation (see, for example, Hottel and Sarofim [8], Penner and Olfe [9], Dalzell and Sarofim [10], Siegel and Howell [11], Thring and Lowes [12], Felske and Tien [13], Buckius and Tien [14], Sarofim and Hottel [15], Tien and Lee [16], Bard and Pagni [17], Santoro *et al.* [18], and Beier *et al.* [19]). This approximation is usually assumed to be accurate up to the size parameter $\alpha = \pi D/\lambda \cong 0.3$, D being the particle diameter, λ the wavelength of radiation. Kerker *et al.* [20], Bayvel and Jones [6], and Ku and Felske [21] have recently contributed to improvements on this criterion. The first objective of the present study is to use the Penndorf correction and contribute further to this criterion as applied to combustion and heat transfer. The second objective is to demonstrate the effect of Penndorf correction on the Planck mean and the Rosseland mean absorption coefficients based on the Rayleigh limit. Here a brief review of Penndorf [22, 23] and Ku and Felske [21] will prove convenient later.

Penndorf [22, 23] considered non-absorbing particles with $1.05 \leqslant n \leqslant 2.0$, and absorbing particles with $n = 1.29$, and discrete k values in the range $0.0645 \leqslant k \leqslant 5.16$, and with $n = 1.25$, 1.50, 1.75, and discrete k values in the range $0.125 \leqslant k \leqslant 1.05$, n and k being refractive and absorptive indices, respectively. He presented curves of constant percent error for various limiting approximations in the α–n domain. Ku and Felske [21] studied the range of refractive indices $1.01 \leqslant n \leqslant 50$ and $0 \leqslant k \leqslant 50$ with results up to $n = k = 1600$ in some cases. They numerically evaluated α values below which Rayleigh and Penndorf expressions for scattering and extinction

NOMENCLATURE

a, b	expansion coefficients defined by equations (4e) and (4f)
c	speed of light, 2.9979×10^8 m s^{-1}
C	cross section [m^2]
C_1	first radiation constant, 3.74×10^{-16} W m^2
C_2	second radiation constant, 1.4388×10^{-2} m K
D	diameter [m]
$E_{b\lambda}$	emissive power of blackbody [W m^{-3}]
f_v	soot volume fraction [m^3 particle m^{-3}]
h	Planck's constant, 6.6262×10^{-34} J s
i	complex unit
$\mathscr{I}$	'the imaginary part of'
k	absorptive index
ℓ	Boltzmann's constant, 1.3806×10^{-23} J K^{-1}
ℓ	summation index
m	complex refractive index
n	refractive index
M_j, N_j	functions of n and k defined following equations (6), (7), (26), and (29)
N	particle number density [number of particles m^{-3}]
P	normalized size distribution function [m^{-1}]
Q	efficiency factor
$\mathscr{R}$	'the real part of'
s	argument of Riemann zeta and Gamma function
T	temperature [K]
V	volume [m^3]
x	integration variable of Riemann zeta function.

Greek symbols

α	size parameter defined by equation (4d)
β	$m\alpha$
Γ	Gamma function
ε	photon energy [J]
ζ	Riemann zeta function
κ	volumetric spectral coefficient [m^{-1}]
κ_P	Planck mean coefficient [m^{-1}]
κ_R	Rosseland mean coefficient [m^{-1}]
λ	wavelength [m]
ν	frequency [s^{-1}]
ξ	Riccati–Bessel functions
Ξ	function defined by equation (14)
Π	Penndorf correction
ψ	Riccati–Bessel functions.

Subscripts

a	absorption
b	blackbody
e	extinction
λ	spectral
p	particle
P	Planck mean absorption coefficient
R	Rosseland mean absorption coefficient
s	scattering.

Superscripts

E	Exact
P	Penndorf
R	Rayleigh
$'$	differentiation with respect to the argument.

efficiencies are accurate within 1% of the LM theory. The present study, following the illustration of error variation as a continuous function of the size parameter, considers the range $1.5 \leqslant n \leqslant 2.5$, $0.5 \leqslant k \leqslant 1.5$ which is important for combustion and heat transfer; it includes higher attainable quantities of error, and shows the need of the Penndorf correction on the Planck mean and the Rosseland mean absorption coefficients for large particle clouds. Needless to say, the prime motivation for studying the Rayleigh and Penndorf limits is not because these limits provide any substantial computational saving as opposed to direct LM theory computations but because they provide explicit analytical expressions which are convenient to use (see, for example, refs. [8–19]).

The study consists of six sections: following this introduction, Section 2 relates efficiency factors and cross sections to spectral coefficients, expresses efficiency factors for LM theory, and derives the Rayleigh and Penndorf limits of these factors. Section 3 applies these approximations to soot and establishes the upper bounds for a discrete set of m by introducing a predefined error relative to the LM theory. This is followed by the generation of error contours for both the Rayleigh and Penndorf approximations in the n–k domain as continuous functions of m and discrete functions of α. Section 4 illustrates the importance of Penndorf expansion in terms of three practical problems, two involving optical diagnostics (OD) and one involving radiative heat transfer (RHT). Section 5 develops the Planck mean and the Rosseland mean absorption coefficients in terms of the Penndorf expansion, and Section 6 concludes the study.

2. PENNDORF CORRECTION

Under the assumptions of single and independent scattering, the spectral coefficients of the radiative transfer equation (RTE) for a polydisperse media (see, for example, Buckius and Hwang [24], and Mengüç and Viskanta [25]) are

$$\kappa_{a,s}(m,N,\lambda) = \int_0^\infty Q_{a,s}(m,D,\lambda)\frac{\pi D^2}{4}NP(D)\,d(D) \quad (1)$$

and

$$\kappa_e(m,N,\lambda) = \kappa_a(m,N,\lambda)+\kappa_s(m,N,\lambda) \quad (2)$$

where subscripts a, s, and e denote absorption, scattering, and extinction, respectively, $m = n-ik$ is the usual complex refractive index of particles with respect to the surrounding medium, i the complex unit, N the particle number density, Q the efficiency factor, and $P(D)$ the normalized particle size distribution function which satisfies

$$\int_0^\infty P(D)\,d(D) = 1.$$

For a monodisperse medium, equations (1) and (2) are reduced, in terms of the definition of the cross section $C = Q(\pi D^2/4)$, to

$$\kappa_{a,s,e} = Q_{a,s,e}\frac{\pi D^2}{4}N \equiv C_{a,s,e}N. \quad (3)$$

The LM theory derived for isotropic, homogeneous spheres gives for the extinction and scattering efficiencies (refer to, for example, van de Hulst [1])

$$Q_e(m,D,\lambda) = \frac{2}{\alpha^2}\sum_{\ell=1}^{\infty}(2\ell+1)\mathscr{R}(a_\ell+b_\ell) \quad (4a)$$

$$Q_s(m,D,\lambda) = \frac{2}{\alpha^2}\sum_{\ell=1}^{\infty}(2\ell+1)(|a_\ell|^2+|b_\ell|^2) \quad (4b)$$

and for the absorption efficiency

$$Q_a(m,D,\lambda) = Q_e(m,D,\lambda)-Q_s(m,D,\lambda) \quad (4c)$$

where

$$\alpha = \frac{\pi D}{\lambda} \quad (4d)$$

is the size parameter and $\mathscr{R}$ indicates 'the real part of', $|\,|$ 'the absolute value of', a_ℓ and b_ℓ are the expansion coefficients (see, for example, p. 123 of van de Hulst [1], and p. 45 of Kerker [2])

$$a_\ell = a_\ell(\alpha,m) = \frac{\psi_\ell(\alpha)[\psi'_\ell(\beta)/\psi_\ell(\beta)]-m\psi'_\ell(\alpha)}{\xi_\ell(\alpha)[\psi'_\ell(\beta)/\psi_\ell(\beta)]-m\xi'_\ell(\alpha)} \quad (4e)$$

$$b_\ell = b_\ell(\alpha,m) = \frac{m\psi_\ell(\alpha)[\psi'_\ell(\beta)/\psi_\ell(\beta)]-\psi'_\ell(\alpha)}{m\xi_\ell(\alpha)[\psi'_\ell(\beta)/\psi_\ell(\beta)]-\xi'_\ell(\alpha)} \quad (4f)$$

where $\beta = m\alpha$, and ψ, ξ are the Riccati–Bessel functions, and the prime denotes differentiation with respect to the argument. Equations (3) and (4) coupled with information on N allow the computation of spectral coefficients.

In the Rayleigh limit where $\alpha \ll 1$, the efficiency factors are known to be (see, for example, van de Hulst [1])

$$Q_a^R(m,\alpha) = -4\alpha\mathscr{I}\left(\frac{m^2-1}{m^2+2}\right),\quad Q_s^R(m,\alpha) = \tfrac{8}{3}\alpha^4\left|\frac{m^2-1}{m^2+2}\right|^2 \quad (5a,b)$$

and

$$Q_e^R(m,\alpha) = Q_a^R(m,\alpha)+Q_s^R(m,\alpha) \quad (5c)$$

where superscript R is for Rayleigh; $\mathscr{I}$, 'the imaginary part of'. Insertion of $m = n-ik$ into equations (5a) and (5b) yields explicit expressions for efficiency factors in terms of α, n, and k. These are

$$Q_a^R = 12\left(\frac{N_1}{M_1}\right)\alpha,\quad Q_s^R = \frac{8}{3}\left(1-3\frac{M_2}{M_1}\right)\alpha^4 \quad (6a,b)$$

and

$$Q_e^R = Q_a^R+Q_s^R \quad (6c)$$

where

$$M_1 = N_1^2+(2+N_2)^2,\quad M_2 = 1+2N_2$$

and

$$N_1 = 2nk,\quad N_2 = n^2-k^2.$$

The foregoing results have been extended by Penndorf [22, 23, 26] to larger particles. He performed a series expansion of a_ℓ and b_ℓ containing α up to α^7 for both Q_e and Q_s ($\ell = 1,2,3$) in the case of absorbing particles (see Table III in ref. [22]). Following the insertion of coefficients to the efficiency factors (given by equations (4a) and (4b)), he obtained the series expansion with α^5 truncated in Q_e and α^8 and higher order terms truncated† in Q_s. For scattering and extinction efficiency factors, the Penndorf expansion can be expressed, after some rearrangement, as

$$Q_s^P = Q_s^R\left[1+2\frac{\alpha^2}{M_1}(\tfrac{3}{5}M_3-2N_1\alpha)\right] \quad (7a)$$

† Here, some remarks on the literature may prove convenient for future studies. Caution should be exercised when truncated terms such as α^5 in Q_e, and α^8 and higher order terms in Q_s are considered. These involve R and T definitions given by Penndorf [22] in his Table II. The R_1, T_1 and R_2, T_2 expressions defined as real and imaginary parts of R and T appear to be inconsistent with R and T. Since these higher order terms are not used here or elsewhere [6, 21], no error is introduced. However, in the Penndorf expansion given by Bayvel and Jones [6], the sign of $36n^2k^2$ needs to be minus to be consistent with the original expression given by Penndorf [22, 23, 26]. This sign change eliminates the apparent equality of α^4-related terms in Q_s and Q_e as claimed by Bayvel and Jones [6].

$$Q_e^P = Q_a^R + 2\alpha^3\left[N_1\left(\frac{1}{15}+\frac{5}{3}\frac{1}{M_4}+\frac{6}{5}\frac{M_5}{M_1^2}\right) + \frac{4}{3}\frac{M_6}{M_1^2}\alpha\right] \quad (7b)$$

and

$$Q_a^P = Q_e^P - Q_s^P \quad (7c)$$

where superscript P is for Penndorf, and the remaining Ms are defined as

$$M_3 = N_3 - 4, \quad M_4 = 4N_1^2 + (3+2N_2)^2$$

$$M_5 = 4(N_2-5)+7N_3, \quad M_6 = (N_2+N_3-2)^2 - 9N_1^2$$

and

$$N_3 = (n^2+k^2)^2 = N_1^2 + N_2^2.$$

The practical significance of the Penndorf correction for some radiation problems is demonstrated in the following sections.

3. PARTICULATE LADEN HEAT TRANSFER AND COMBUSTION

The LM theory and its Rayleigh limit have been extensively used in combustion problems involving RHT and/or OD. The majority of OD studies on combustion attempt to extract information about the properties of combustion generated particles such as soot formed by burning of hydrocarbon (HC) fuels. The soot is distinguished here from other carbon-related structures such as graphite and carbon black by its content of some soluble organic fraction [27, 28] and its structure which involves a substantial number of small crystallites as demonstrated by Lahaye and Prado [29], each crystallite has 3–5 turbostratic layers, that is, carbon atoms in layers of hexagons and layers disoriented by random rotations separated by 3.44 Å as stated by Palmer and Cullis [30] (quoted also in Glassman [31]). Depending on the chemical composition and HC content, the refractive and absorptive indices of soot are experimentally found to fall into $1.5 \leqslant n \leqslant 2.5$ and $0.5 \leqslant k \leqslant 1.5$ in the visible range [32]. The larger values generally correspond to higher content of pure carbon (see, for example, Roessler *et al.* [33] for a model illustrating the effect of HCs on the soot refractive index). In RHT studies, the properties of soot in the near infra-red (say 1–5 μm for typical temperatures) also become important. Although n and k depend on the wavelength [34–38], this dependence remains well within the spread of the experimental data in the visible range. An inspection of heat transfer and combustion literature [10, 16, 32, 36, 39–43] reveal three widely used complex refractive indices

$m = 1.5-0.5\text{i}$ (Dalzell and Sarofim [10])

$m = 2.0-1.0\text{i}$ (Janzen [32])

$m \cong 1.75-0.75\text{i}$ (Pluchino *et al.* [39])

the first two being the lower and upper bounds and the third one being the separate arithmetic average of the real and imaginary parts of the first two. These indices approximately cover the variation in both visible and near infra-red.

Exact LM calculations for equations (4a)–(4c) require the evaluation of a_ℓ and b_ℓ from equations (4e) and (4f) which can be reduced to a combination of half integer order Bessel functions with real and complex arguments. Several techniques for the computation of expansion coefficients are described in Kerker [2] and in the studies by Aden [44], Dave [45], Verner [46], Lentz [47, 48], Grehan and Gousbet [49], Jones [50], and Wiscombe [51, 52]. Aden and Dave utilize logarithmic derivatives of Riccati–Bessel functions which are related by recursive relations. Verner derives a recursion formula for a Wronskian and a function involving Riccati–Bessel functions. Lentz, Grehan and Gousbet, and Jones deal with the ratios of functions making use of continued fractions. Wiscombe improves the available algorithms by developing efficient recurrence formulas for angular functions and by generating an empirical criterion for allowing up-recurrence in the computation of half order Bessel functions. A realistic comparison of Dave's and Wiscombe's algorithms has been made by Felske *et al.* [53]. In the present study, in accordance with the Wiscombe criterion [51, 52] and the Dave study [45], computations with a fast up-recurrence scheme are carried out in the specified ranges of m and α (see, also, Selamet [54]). Figure 1 shows the extinction efficiency vs the particle size parameter for three values of m. However, hereafter the discussion will be carried out only in terms of $m = 2-\text{i}$ because of its algebraic simplicity and frequent use in the literature. Figure 2 illustrates the deviation of the Rayleigh limit and the Penndorf extension from the LM theory for one refractive index typical for soot. The figure clearly demonstrates the importance of the Penndorf correction on the Rayleigh limit.

Let the error in the Rayleigh limit and the Penndorf extension be defined as

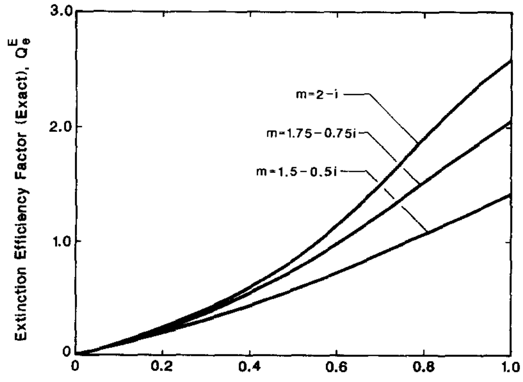

FIG. 1. The extinction efficiency factor from LM theory vs the size parameter for typical values of m.

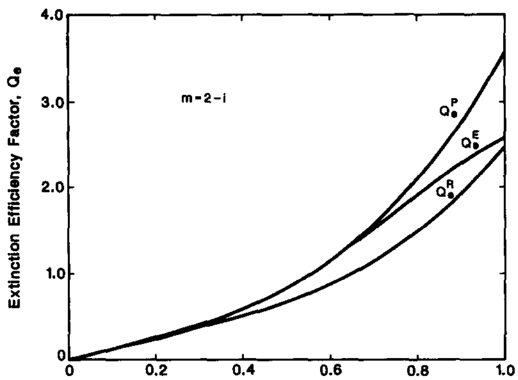

FIG. 2. The extinction efficiency factor vs the size parameter, from LM theory, Rayleigh and Penndorf approximations.

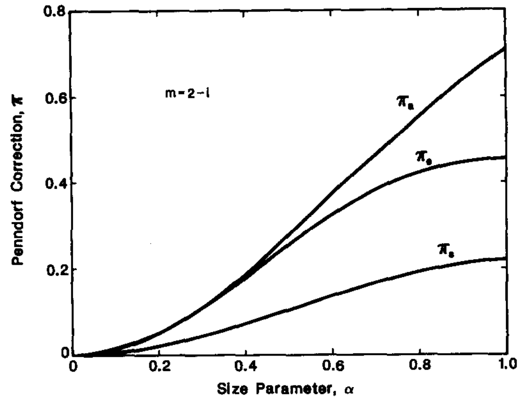

FIG. 4. The Penndorf correction for absorption, extinction and scattering vs the size parameter.

$$|\text{Error}|\ \% = \frac{|Q_e^{R\,\text{or}\,P} - Q_e^E|}{Q_e^E} \times 100$$

where superscript E is for the exact solution. In Fig. 3, this error is plotted against α for $m = 2-i$. The results show the following.

(1) Penndorf error, in the domain of interest, is negligibly small for $\alpha \leqslant 0.6$ (twice the value usually suggested for the Rayleigh limit). For $\alpha = 0.7$, for example, $|\text{Error}|^R = 25.3\%$, whereas $|\text{Error}|^P \cong 3.3\%$. To match the error of the Rayleigh limit to that of the Penndorf expansion, the size parameter has to be limited to $\alpha \cong 0.16$!

(2) For an error of 10% in the extinction efficiency, the upper Rayleigh and Penndorf bounds are $\alpha^R \cong 0.3$ and $\alpha^P \cong 0.8$, approximately.

(3) For all three values of m considered above, the upper bounds of particle size are $\alpha^R \leqslant 0.3$ and $\alpha^P \leqslant 0.75$ for an error of less than 10%.

Let the Penndorf correction on the Rayleigh limit be conveniently expressed as

$$Q^P_{a,s,e} = Q^R_{a,s,e}(1 + \Pi_{a,s,e}) \tag{8}$$

where, in view of equation (4c)

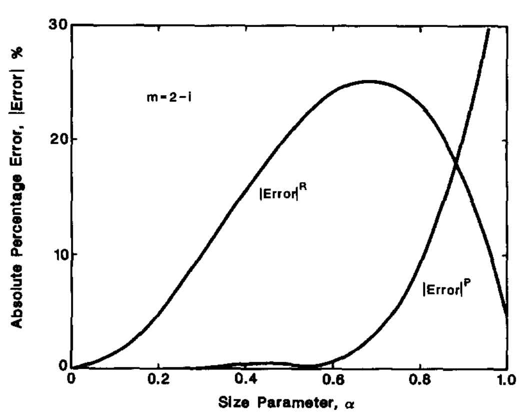

FIG. 3. The absolute percentage error for Rayleigh and Penndorf approximations vs the size parameter.

$$\Pi_e = \left(\frac{Q_a^R}{Q_e^R}\right)\Pi_a + \left(\frac{Q_s^R}{Q_e^R}\right)\Pi_s \tag{9}$$

Π denoting the Penndorf correction on the Rayleigh limit. These corrections are plotted in Fig. 4 for one refractive index. Higher values for absorption and extinction corrections as opposed to that of scattering may be attributed to lower (α^3, α^4)-power contributions to the former two and higher (α^6, α^7)-power contributions to the latter.

Note that the four figures considered so far are all based on the discrete m values. Although some useful results are generated, the variation of error as a function of n and k remains untreated. In previous studies, for example, Kerker *et al.* [20] investigated the Rayleigh error in the n–k domain, plotting a 1% error contour for discrete size parameters in the range $0.01 \leqslant \alpha \leqslant 0.11$ for varying n and k in the range $1 < n < 100$ and $0 < k < 1000$; as previously mentioned, Ku and Felske [21] obtained α below which 1% accuracy in efficiency factors is ensured for the Rayleigh and Penndorf errors in the α–n domain for $1.01 \leqslant n \leqslant 50$ and $0 \leqslant k \leqslant 50$. In some applications, however, an error reasonably higher than 1% may be allowed for a maximum benefit from the use of the Rayleigh limit or the Penndorf correction; also, the range of interest for α is more towards the upper bounds which may exceed 0.11, the largest size parameter considered by Kerker *et al.* [20]. Thus, for $\alpha = 0.3$, 0.5, and 0.7, and as continuous functions of n and k in the ranges $1.5 \leqslant n \leqslant 2.5$ and $0.5 \leqslant k \leqslant 1.5$, the error contours are generated for the Rayleigh and Penndorf based extinction efficiencies (Figs. 5 and 6). Both figures demonstrate stronger error dependence on n than on k which implies that for a given $|m|$ markedly different errors may result depending on the relative magnitudes of n and k. Consequently, the use of an error criterion based on $|m|$ may needlessly lower the permissible upper limit of the size parameter. This fact can also be seen from Fig. 4 of Ku and Felske's study [21] which shows almost an order of magnitude scattering corresponding to an assumed 1% error for

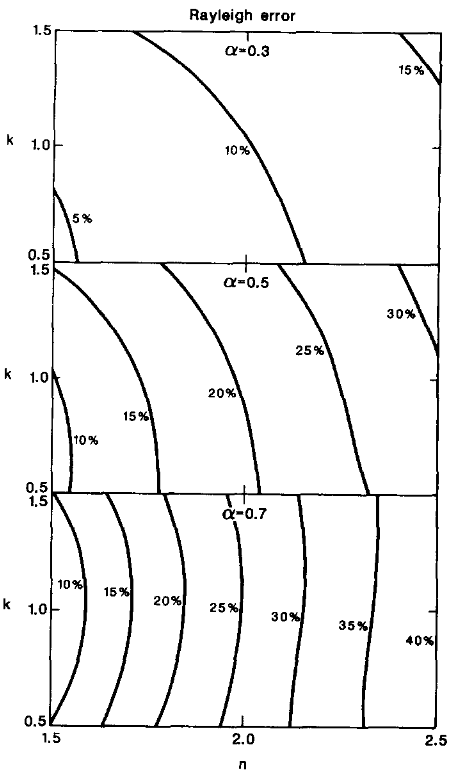

FIG. 5. The error contours for extinction efficiency in the Rayleigh limit for size parameters $\alpha = 0.3, 0.5, 0.7$.

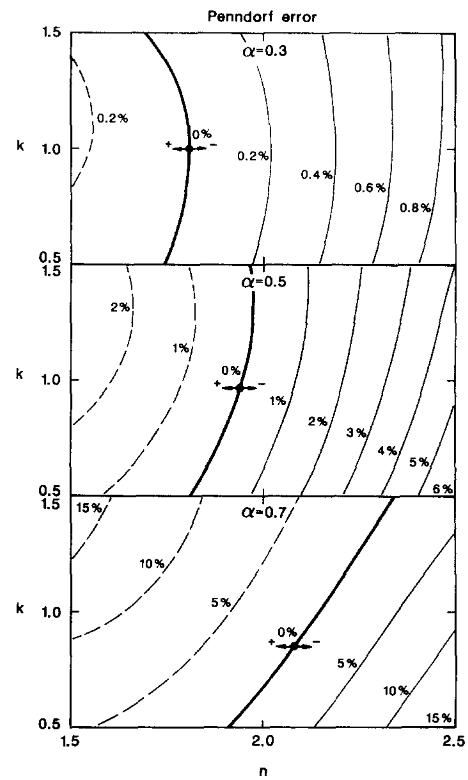

FIG. 6. The error contours for extinction efficiency in the Penndorf correction for size parameters $\alpha = 0.3, 0.5, 0.7$.

fixed $|m|$. Their study suggests the need for error contours for specific ranges of m which are provided by Figs. 5 and 6. Note that for $\alpha = 0.3$, while the maximum Rayleigh error is more than 15% in Fig. 5, the maximum Penndorf error is less than 1%. Likewise, for $\alpha = 0.5$, the Rayleigh error may exceed 30% whereas the Penndorf error is limited to 6%. Finally, for $\alpha = 0.7$, the Rayleigh error reaches 40% whereas the Penndorf error remains within 15%. Also consistent with Fig. 3, and for $m = 2 - \mathrm{i}$, the Rayleigh error exceeds 20%, while the Penndorf error remains less than 1%.

4. APPLICATIONS TO OPTICAL DIAGNOSTICS AND RADIATIVE HEAT TRANSFER

This section is devoted to an illustration on the practical significance of the Penndorf correction in some problems of optical diagnostics and radiative heat transfer.

Light scattering experiments are usually performed with a He–Ne laser at $\lambda_{\mathrm{He\text{-}Ne}} = 632.8$ nm (red) for extinction and with an argon ion (Ar^+) laser at $\lambda_{Ar^+,1} = 488$ nm (blue) and $\lambda_{Ar^+,2} = 514.5$ nm (green) for scattering. For example, consider $\lambda_{\mathrm{He\text{-}Ne}}$ for an illustration on particle size. The size of soot particles are known experimentally to vary in a range, say from 500 Å up to ~2500 Å [41, 42, 55]. Accordingly, the limits of α are

$$\frac{500\pi}{6328} = 0.25 < \alpha < 1.24 = \frac{2500\pi}{6328}. \qquad (10)$$

Thus, up to $D \cong 500$ Å, the Rayleigh limit can be safely used. Beyond this size, however, and up to $D \cong 1500$ Å, the Penndorf correction needs to be taken into account. The actual particle size in the majority of experiments, unless there is a substantial coagulation and agglomeration, turns out to remain within the latter limit.

For another illustration on particle size, assume the particle radiation to be spectrally continuous and be represented by the Planck distribution. For typical flame temperatures (1500–2000 K), about 90% of the radiation emitted from flames is then contained in a wavelength range of 1–5 μm. In this range and even for a reasonably large particle size, say $D = 2500$ Å, the size parameter turns out to be

$$\frac{2500\pi}{50\,000} \cong 0.16 < \alpha < 0.79 \cong \frac{2500\pi}{10\,000} \qquad (11)$$

which shows that, in a radiating flame, the large particles are covered by the Penndorf expansion.

For an illustration on optical diagnostics, consider one of the typical OD experiments which involves laser beam (say, He–Ne with $\lambda_{\mathrm{He\text{-}Ne}} = 632.8$ nm) attenuation through a particulate laden medium of known optical path length. The usual objective of such an experiment is to determine the spectral extinction coefficient, the extinction cross section and the num-

Table 1. Comparison of approximations with the LM theory

	LM theory	Penndorf	Rayleigh	$\lvert\text{Error}\rvert^{P}$ %	$\lvert\text{Error}\rvert^{R}$ %
Q_e	1.147	1.153	0.871	0.48	24.0
$C_e \times 10^{14}$	1.298	1.304	0.985	0.48	24.0
$N \times 10^{-14}$	3.852	3.835	5.076	0.44	31.8
$f_v \times 10^{7}$	3.485	3.471	4.593	0.44	31.8

ber density (or the soot volume fraction). Let the particle size be uniform and known, say $D = 1200$ Å. For a homogeneous, isothermal, and attenuating cold medium, the RTE is simplified to Beer's law. Insertion of the measured path length and the incident and transmitted intensities into the foregoing law yields the spectral extinction coefficient κ_e. Note that the spectral extinction coefficients may vary by several orders of magnitude, depending on the wavelength, the type of combustion (diffusion or premixed), the stoichiometric ratio if premixed, the type of reactants, and the location. A recent spectroscopic study by Hamadi *et al.* [56], for example, reports radiation from premixed flat flames of methane–oxygen and propane–oxygen in a wavelength range 0.4–5 μm. Depending on the stoichiometric ratio and the height in the flame, and for $\lambda = 632.8$ nm, their study gives $\kappa_e \cong 0.2$–$6.5\ \mathrm{m}^{-1}$ and 2–25 m^{-1} for methane and propane, respectively. This suggests the use of a typical value of $\kappa_e = 5\ \mathrm{m}^{-1}$ in the following illustration.

The size parameter, in view of $D = 1200$ Å and $\lambda = 6328$ Å, is

$$\alpha = \frac{\pi D}{\lambda} = 0.6.$$

Assuming $m = 2 - \mathrm{i}$, the extinction efficiency is obtained from the LM code [54] to be

$$Q_e \cong 1.147\ [\text{dimensionless}].$$

Also, from the definition of cross section

$$C_e = \frac{\pi D^2}{4} Q_e \cong 1.298 \times 10^{-14}\ \mathrm{m}^2.$$

In terms of $\kappa_e = 5\ \mathrm{m}^{-1}$, the LM theory yields for the particle number density N (recall equation (3))

$$N = \frac{\kappa_e}{C_e} = \frac{5.0}{1.298 \times 10^{-14}}$$

$$= 3.852 \times 10^{14} \left[\frac{\text{number of particles}}{\mathrm{m}^3}\right].$$

In terms of the soot volume fraction $f_v = NV_p$, V_p being the volume of a single particle

$$f_v = N\frac{\pi D^3}{6} \cong 3.49 \times 10^{-7} \left[\frac{\mathrm{m}^3\ \text{particle}}{\mathrm{m}^3}\right]$$

or, the particle mass concentration which can be readily obtained by multiplying f_v with the particle density.

The foregoing calculations have also been performed by the Rayleigh and Penndorf approximations, employing, respectively, equations (6) and (7). Results given in Table 1 show the markedly higher accuracy of the Penndorf approximation relative to the Rayleigh approximation, as expected.

5. MODIFIED PLANCK AND ROSSELAND MEAN ABSORPTION COEFFICIENTS

The spectral properties of radiation such as spectral coefficients of RTE and spectral emissivity for a homogeneous, isothermal medium derived by employing the Rayleigh limit are available in the literature. Similar studies can be carried out in terms of the Penndorf expansion. However, in a particulate medium exhibiting continuous radiation, spectrally integrated quantities are needed. Two such quantities are the Planck mean and the Rosseland mean absorption coefficients (see, for example, Sparrow and Cess [57])

$$\kappa_P = \frac{\int_0^\infty \kappa_{a\lambda} E_{b\lambda}\, \mathrm{d}\lambda}{\int_0^\infty E_{b\lambda}\, \mathrm{d}\lambda} \tag{12}$$

and

$$\kappa_R = \frac{\int_0^\infty \frac{\partial E_{b\lambda}}{\partial T}\, \mathrm{d}\lambda}{\int_0^\infty \frac{1}{\kappa_{a\lambda}} \frac{\partial E_{b\lambda}}{\partial T}\, \mathrm{d}\lambda} \tag{13}$$

where $E_{b\lambda}$ is the spectral Planck function for blackbody emissive power. The Planck and Rosseland mean coefficients derived analytically by Felske and Tien [58] for the Rayleigh limit motivates the following development on these coefficients from the Penndorf expansion which covers the larger soot particles discussed in the previous section. Inserting

$$N = \frac{f_v}{\pi D^3/6}$$

into equation (3) and combining with equation (7) for Q_a yields the following expression for the spectral absorption coefficient based on the Penndorf expansion:

$$\kappa_{a\lambda}^{P} = \left(18\pi \frac{N_1}{M_1} f_v\right)\frac{1}{\lambda} + \left[N_1\left(\frac{1}{5} + \frac{5}{M_4} + \frac{18}{5}\frac{M_5}{M_1^2}\right)\pi^3 D^2 f_v\right]\frac{1}{\lambda^3} + \left[4\left(\frac{M_6}{M_1^2} - 1 + 3\frac{M_2}{M_1}\right)\pi^4 D^3 f_v\right]\frac{1}{\lambda} \tag{14}$$

where the first term represents the Rayleigh contribution to be denoted by $\kappa_{a\lambda}^{R}$. In the development of this relation, two highest order terms introduced by $Q_s(\alpha^6, \alpha^7)$ are neglected, an omission which is numerically justified.

To proceed with the development of the Penndorf based Planck mean absorption coefficient, substitute equation (14) into equation (12) and transform the integration in the latter equation in terms of $x = h\nu/\ell T = C_2/\lambda T$, h being Planck's constant, ν the frequency, ℓ Boltzmann's constant, T the temperature, and $C_2 = hc/\ell$ the second radiation constant, c being the speed of light, to obtain

$$\kappa_P^P = 18\frac{\Xi(5)}{\Xi(4)}\frac{N_1}{M_1}f_v\left(\frac{\pi T}{C_2}\right) + \frac{\Xi(7)}{\Xi(4)}N_1\left(\frac{1}{5}+\frac{5}{M_4}+\frac{18}{5}\frac{M_5}{M_1^2}\right)f_vD^2\left(\frac{\pi T}{C_2}\right)^3 + 4\frac{\Xi(8)}{\Xi(4)}\left(\frac{M_6}{M_1^2}-1+3\frac{M_2}{M_1}\right)f_vD^3\left(\frac{\pi T}{C_2}\right)^4 \quad (15)$$

where $\Xi(s)$ is defined as

$$\Xi(s) = \zeta(s)\Gamma(s) = \int_0^\infty \frac{x^{s-1}}{e^x-1}\,dx \quad (16)$$

ζ being the Riemann zeta function [59], and Γ the Gamma function; and others have dimensions C_2 [m K], T [K], D [m], and κ_P^P [m^{-1}]. Following appropriate integrations, the Planck mean absorption coefficient based on the Penndorf expansion is found to be

$$\kappa_P^P = 68.98\frac{N_1}{M_1}f_v\left(\frac{\pi T}{C_2}\right) + 111.8N_1\left(\frac{1}{5}+\frac{5}{M_4}+\frac{18}{5}\frac{M_5}{M_1^2}\right)f_vD^2\left(\frac{\pi T}{C_2}\right)^3 + 3117\left(\frac{M_6}{M_1^2}-1+3\frac{M_2}{M_1}\right)f_vD^3\left(\frac{\pi T}{C_2}\right)^4 \quad (17)$$

where the first term

$$\kappa_P^R = 3.8322\left(18\frac{N_1}{M_1}\right)f_v\left(\frac{\pi T}{C_2}\right) \quad (18)$$

is the Planck mean absorption coefficient based on the Rayleigh limit, originally derived by Felske and Tien [58]. Equation (17) can be rearranged as

$$\frac{\kappa_P^P}{\kappa_P^R} = 1 + 1.6207M_1\left(\frac{1}{5}+\frac{5}{M_4}+\frac{18}{5}\frac{M_5}{M_1^2}\right)\left(\frac{\pi DT}{C_2}\right)^2 + 45.1882\frac{M_1}{N_1}\left(\frac{M_6}{M_1^2}-1+3\frac{M_2}{M_1}\right)\left(\frac{\pi DT}{C_2}\right)^3 \quad (19a)$$

or

$$\kappa_P^P/\kappa_P^R = 1 + \Pi_P^P(\underbrace{M_1,\ldots,N_1,\ldots,}_{\text{EM waves}}\ \underbrace{\pi DT/C_2}_{\text{Quanta}}) \quad (19b)$$

where Π_P is the Penndorf correction to the Rayleigh based Planck mean absorption coefficient. This correction depends on Ms and Ns (given in terms of n and k) and the dimensionless $\pi DT/C_2$ (combining the effects of diameter and temperature). The former shows the mean effect of the interaction of electromagnetic waves with spherical particles, while the physical significance of the latter is clear from quantum mechanics; recalling that the radiation–matter interaction is mostly between photons and the vibrational mode of matter [60, 61], consider the photon energy ε relative to the mean energy ℓT of the harmonic oscillator

$$\varepsilon/\ell T \quad (20)$$

which may be rearranged for a photon of frequency ν as

$$h\nu/\ell T \quad (21)$$

or, in terms of wavelength $\lambda = c/\nu$, as

$$C_2/\lambda T \quad (22)$$

where c is the speed of light. On dimensional grounds, combining equation (22) with the definition of the size parameter as

$$C_2/\lambda T \sim \pi D/\lambda \quad (23)$$

readily yields

$$\pi DT/C_2. \quad (24)$$

Now, proceed to the development of the Rosseland mean absorption coefficient. The numerator of equation (13) readily yields

$$\int_0^\infty \frac{\partial E_{b\lambda}}{\partial T}\,d\lambda = \frac{C_1T^3}{C_2^4}\int_0^\infty \frac{x^4e^x}{(e^x-1)^2}\,dx$$

or, following an integration by parts and in view of equation (16)

$$\int_0^\infty \frac{\partial E_{b\lambda}}{\partial T}\,d\lambda = 4\Xi(4)\frac{C_1T^3}{C_2^4}. \quad (25)$$

For integration of the denominator of equation (13), first rearrange the reciprocal of $\kappa_{a\lambda}^P$ as

$$\frac{1}{\kappa_{a\lambda}^P} = \frac{1}{\kappa_{a\lambda}^R}\frac{1}{[1+M_I\alpha^2+M_{II}\alpha^3]} \quad (26)$$

where M_I and M_{II} are defined as

$$M_I = \frac{M_1}{18}\left(\frac{1}{5}+\frac{5}{M_4}+\frac{18}{5}\frac{M_5}{M_1^2}\right)$$

$$M_{II} = \frac{2}{9}\frac{M_1}{N_1}\left(\frac{M_6}{M_1^2}-1+3\frac{M_2}{M_1}\right).$$

For $M_I = 0$ and $M_{II} = 0$, the denominator of equation (13) yields

$$\int_0^\infty \frac{1}{\kappa_{a\lambda}^R}\frac{\partial E_{b\lambda}}{\partial T}\mathrm{d}\lambda = 3\Xi(3)\frac{C_1}{18\pi\frac{N_1}{M_1}f_v}\frac{T^2}{C_2^3} \quad (27)$$

which, in view of equations (13) and (25), gives the Rosseland mean absorption coefficient based on the Rayleigh limit

$$\kappa_R^R = 3.6016\left(18\frac{N_1}{M_1}\right)f_v\left(\frac{\pi T}{C_2}\right) \quad (28)$$

originally derived by Felske and Tien [58]. When M_I and M_{II} in equation (26) are taken into account a closed form integration of the denominator of equation (13) does no longer appear to be feasible. To circumvent this difficulty, assume

$$\frac{1}{[1+M_I\alpha^2+M_{II}\alpha^3]} \cong 1+M_{III}\alpha^2+M_{IV}\alpha^3 \quad (29)$$

where the right-hand side already satisfies the approximated function and its derivative for $\alpha = 0$. Considering the range of interest for the size parameter, satisfy equation (29) also at $\alpha = 0.4$ and 0.8. Then M_{III} and M_{IV} become

$$M_{III} \cong -10.9375\left[1-\frac{1+0.70857M_I+0.576M_{II}}{(1+0.16M_I+0.064M_{II})(1+0.64M_I+0.512M_{II})}\right]$$

and

$$M_{IV} \cong 11.71875\left[1-\frac{1+0.8M_I+0.6613M_{II}}{(1+0.16M_I+0.064M_{II})(1+0.64M_I+0.512M_{II})}\right].$$

The maximum discrepancy introduced by the approximation on the right-hand side of equation (26) remains within 1% of the left-hand side of the same equation for the range of m of interest and $0 \leqslant \alpha \leqslant 0.8$. In terms of these approximations the denominator of equation (13) yields

$$\int_0^\infty \frac{1}{\kappa_{a\lambda}^P}\frac{\partial E_{b\lambda}}{\partial T}\mathrm{d}\lambda = \frac{C_1T^2}{18\pi\frac{N_1}{M_1}f_vC_2^3} \times\left[3\Xi(3)+5\Xi(5)M_{III}\left(\frac{\pi DT}{C_2}\right)^2+6\Xi(6)M_{IV}\left(\frac{\pi DT}{C_2}\right)^3\right]. \quad (30)$$

Then, from the combination of equations (13), (25), (27), (28), and (30)

$$\frac{\kappa_R^P}{\kappa_R^R} = \frac{1}{1+\frac{5\Xi(5)}{3\Xi(3)}M_{III}\left(\frac{\pi DT}{C_2}\right)^2+2\frac{\Xi(6)}{\Xi(3)}M_{IV}\left(\frac{\pi DT}{C_2}\right)^3}$$

and evaluation of the Ξ function in terms of Riemann zeta and Gamma functions yields

$$\frac{\kappa_R^P}{\kappa_R^R} = \frac{1}{1+17.253M_{III}\left(\frac{\pi DT}{C_2}\right)^2+101.560M_{IV}\left(\frac{\pi DT}{C_2}\right)^3} \quad (31a)$$

or, introducing Π_R^P

$$\kappa_R^P/\kappa_R^R = 1+\Pi_R^P(\underbrace{M_1,\ldots,N_1,\ldots,}_{\text{EM waves}}\ \underbrace{\pi DT/C_2}_{\text{Quanta}}). \quad (31b)$$

Consider now an illustrative example in terms of $m = 2-i$ from previous sections. The results of calculations for κ_P^P and κ_R^P, respectively, from equations (19a) and (31a) are depicted in Fig. 7 against $\pi DT/C_2$. When the particle diameter is small, the Rayleigh expression is quite adequate; as diameter increases, however, the size parameter in the near infra-red (or, at least, in part of the infra-red) goes beyond the Rayleigh limit as demonstrated in Section 4, and the corrections expressed by equations (19) and (31) are needed. The temperature effect, on the other hand, may be explained by referring to Wien's displacement law. As temperature increases, the distribution shifts towards lower wavelengths forcing a substantial portion of integration in the numerator of equation (12) and in the denominator of equation (13) to be performed at lower wavelengths which implies size parameters exceeding the Rayleigh limit. Figure 7 also illustrates the fact that, although corrections for Planck and Rosseland show a similar trend, the correction to the Rayleigh limit for the Planck mean absorption coefficient is about twice that for the Rosseland mean absorption coefficient.

6. CONCLUSIONS

The Penndorf correction is shown to practically cover the spectral range of continuous radiation from soot particles. The error contours of the extinction

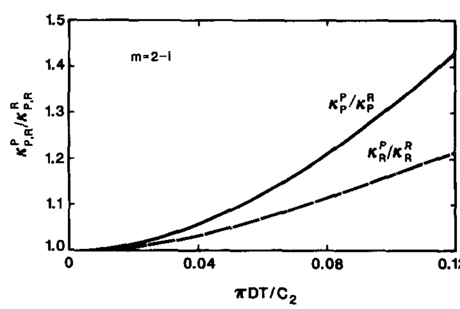

FIG. 7. The Penndorf correction to the Rayleigh based Planck and Rosseland mean coefficients as a function of $\pi DT/C_2$.

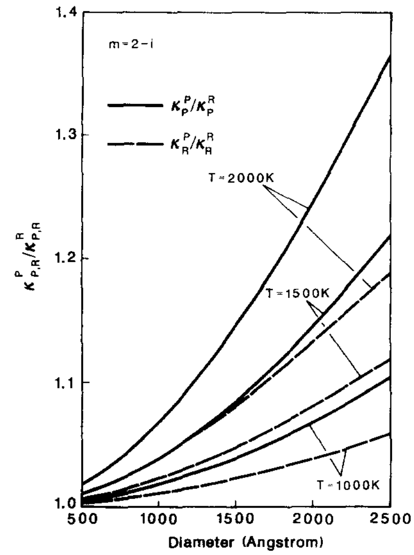

FIG. 8. The Penndorf correction to the Rayleigh based Planck and Rosseland mean coefficients as explicit functions of diameter and temperature.

efficiency factor are generated for the Rayleigh limit and the Penndorf correction for discrete values of size parameter $\alpha = 0.3$, 0.5, 0.7 as a continuous function of n and k in the range $1.5 \leqslant n \leqslant 2.5$ and $0.5 \leqslant k \leqslant 1.5$. For thin clouds, the Penndorf correction is applied to the Planck mean absorption coefficient which yields an expression in terms of refractive and absorptive indices, and $\pi DT/C_2$ [dimensionless]. A similar development is performed for thick clouds leading to an expression for the Rosseland mean absorption coefficient based on the Penndorf correction. Figure 8 is a dimensionally expanded representation of Fig. 7, demonstrating the explicit effects of diameter and temperature in their typical ranges. For the size and temperature ranges considered in this study, equations (19) and (31) should yield results close to the exact integration of equations (12) and (13) because the Penndorf correction covers well the size parameter range of interest. The Rosseland mean for the limit of thick particle cloud needs to be treated with caution because of the single scattering assumed in equations (1)–(3).

REFERENCES

1. H. C. van de Hulst, *Light Scattering by Small Particles*. Wiley, New York (1957).
2. M. Kerker, *The Scattering of Light and Other Electromagnetic Radiation*. Academic Press, New York (1969).
3. D. Deirmendjian, *Electromagnetic Scattering on Spherical Polydispersions*. American Elsevier, New York (1969).
4. M. Born and E. Wolf, *Principles of Optics* (6th Edn). Pergamon Press, Oxford (1986).
5. A. R. Jones, Scattering of electromagnetic radiation in particulate laden fluids, *Prog. Energy Combust. Sci.* **5**, 73–96 (1979).
6. L. P. Bayvel and A. R. Jones, *Electromagnetic Scattering and its Applications*. Applied Science, New Jersey (1981).
7. C. F. Bohren and D. R. Huffman, *Absorption and Scattering of Light by Small Particles*. Wiley, New York (1983).
8. H. C. Hottel and A. F. Sarofim, *Radiative Transfer*, Chap. 12. McGraw-Hill, New York (1967).
9. S. S. Penner and D. B. Olfe, *Radiation and Reentry*, Chap. 4. Academic Press, New York (1968).
10. W. H. Dalzell and A. F. Sarofim, Optical constants of soot and their application to heat flux calculations, *J. Heat Transfer* **91**, 100–104 (1969).
11. R. Siegel and J. R. Howell, *Thermal Radiation Heat Transfer* (2nd Edn), Chap. 17. Hemisphere/McGraw-Hill, Washington, DC (1981).
12. M. W. Thring and T. M. Lowes, Luminous radiation from industrial flames, *Combust. Sci. Technol.* **5**, 251–256 (1972).
13. J. D. Felske and C. L. Tien, Calculation of the emissivity of luminous flames, *Combust. Sci. Technol.* **7**, 25–31 (1973).
14. R. O. Buckius and C. L. Tien, Infrared flame radiation, *Int. J. Heat Mass Transfer* **20**, 93–106 (1977).
15. A. F. Sarofim and H. C. Hottel, Radiative transfer in combustion chambers: influence of alternative fuels, *Proc. 6th Int. Heat Transfer Conf.*, Toronto, Canada, Vol. 6, pp. 199–217 (1978).
16. C. L. Tien and S. C. Lee, Flame radiation, *Prog. Energy Combust. Sci.* **8**, 41–59 (1982).
17. S. Bard and P. J. Pagni, Carbon particulate in small pool fire flames, *J. Heat Transfer* **103**, 357–362 (1981).
18. R. J. Santoro, H. G. Semerjian and R. A. Dobbins, Soot particle measurements in diffusion flames, *Combust. Flame* **51**, 203–218 (1983).
19. R. A. Beier, P. J. Pagni and C. I. Okoh, Soot and radiation in combusting boundary layers, *Combust. Sci. Technol.* **39**, 235–262 (1984).
20. M. Kerker, P. Scheiner and D. D. Cooke, The range of validity of the Rayleigh and Thomson limits for Lorenz–Mie scattering, *J. Opt. Soc. Am.* **68**, 135–137 (1978).
21. J. C. Ku and J. D. Felske, The range of validity of the Rayleigh limit for computing Mie scattering and extinction efficiencies, *J. Quant. Spectrosc. Radiat. Transfer* **31**, 569–574 (1984).
22. R. B. Penndorf, Scattering and extinction coefficients for small absorbing and nonabsorbing aerosols, *J. Opt. Soc. Am.* **52**, 896–904 (1962).
23. R. B. Penndorf, Scattering coefficients for absorbing and nonabsorbing aerosols, Tech. Report RAD-TR-60-27; AFCRL-TN-60-667, Avco Corp., Wilmington, Massachusetts (1960).
24. R. O. Buckius and D. C. Hwang, Radiation properties for polydispersions: application to coal, *J. Heat Transfer* **102**, 99–103 (1980).
25. M. P. Mengüç and R. Viskanta, On the radiative properties of polydispersions: a simplified approach, *Combust. Sci. Technol.* **44**, 143–159 (1985).
26. R. B. Penndorf, Scattering and extinction coefficients for small spherical aerosols, *J. Atmos. Sci.* **19**, 193 (1962).
27. A. G. Gaydon and H. G. Wolfhard, *Flames, Their Structure, Radiation and Temperature*. Chapman & Hall, London (1979).
28. A. I. Medalia, Discussion of ref. [33], p. 89 (1981).
29. J. Lahaye and G. Prado, Morphology and internal structure of soot and carbon blacks. In *Particulate Carbon: Formation During Combustion* (Edited by D. C. Siegla and G. W. Smith), pp. 33–55. Plenum Press, New York (1981).
30. H. B. Palmer and C. F. Cullis, The formation of carbon from gases. In *Chemistry and Physics of Carbon* (Edited by P. L. Walker), Vol. 1, pp. 265–325. Marcel Dekker, New York (1965).
31. I. Glassman, *Combustion* (2nd Edn). Academic Press, New York (1987).

32. J. Janzen, The refractive index of colloidal carbon, *J. Colloid Interface Sci.* **69,** 436–447 (1979).
33. D. M. Roessler, F. R. Faxvog, R. Stevenson and G. W. Smith, Optical properties and morphology of particulate carbon: variation with air/fuel ratio. In *Particulate Carbon: Formation During Combustion* (Edited by D. C. Siegla and G. W. Smith), pp. 57–89. Plenum Press, New York (1981).
34. V. R. Stull and G. N. Plass, Emissivity of dispersed carbon particles, *J. Opt. Soc. Am.* **50,** 121–129 (1960).
35. P. J. Foster and C. R. Howarth, Optical constants of carbon and coals in the infrared, *Carbon* **6,** 719–729 (1968).
36. S. C. Lee and C. L. Tien, Optical constants of soot in hydrocarbon flames, *Eighteenth Symp. (Int.) on Combustion*, pp. 1159–1166. The Combustion Institute, Pittsburgh (1981).
37. S. C. Lee, Q. Z. Yu and C. L. Tien, Radiation properties of soot from diffusion flames, *J. Quant. Spectrosc. Radiat. Transfer* **27,** 387–396 (1982).
38. T. T. Charalampopoulos and J. D. Felske, Refractive indices of soot particles deduced from in-situ laser light scattering measurements, *Combust. Flame* **68,** 283–294 (1987).
39. B. Pluchino, S. S. Goldberg, J. M. Dowling and C. M. Randall, Refractive index measurements of single micron-sized carbon particles, *Appl. Optics* **19,** 3370–3372 (1980).
40. B. L. Drolen and C. L. Tien, Absorption and scattering of agglomerated soot particulate, *J. Quant. Spectrosc. Radiat. Transfer* **37,** 433–448 (1987).
41. A. D'Alessio, Laser light scattering and fluorescence diagnostics of rich flames produced by gaseous and liquid fuel. In *Particulate Carbon: Formation During Combustion* (Edited by D. C. Siegla and G. W. Smith), pp. 207–259. Plenum Press, New York (1981).
42. P. Menna and A. D'Alessio, Light scattering and extinction coefficients for soot forming flames in the wavelength range 0.2μ–0.6μ, *Nineteenth Symp. (Int.) on Combustion*, pp. 1421–1428. The Combustion Institute, Pittsburgh (1982).
43. W. L. Flower, Optical measurements of soot formation in premixed flames, *Combust. Sci. Technol.* **33,** 17–33 (1983).
44. A. L. Aden, Electromagnetic scattering from spheres with sizes comparable to the wavelength, *J. Appl. Phys.* **22,** 601–605 (1951).
45. J. V. Dave, Subroutines for computing the parameters of the electromagnetic radiation scattered by a sphere, Report No. 320–3237, IBM Scientific Center, Palo Alto, California (May 1968). Printed July 1987, IBM Program Information Department, Hawthorne, New York, PID No. 360D-17.4.002.
46. B. Verner, Note on the recurrence between Mie's coefficients, *J. Opt. Soc. Am.* **66,** 1424–1425 (1976).
47. W. J. Lentz, A new method of computing spherical Bessel functions of complex argument with tables, Tech. Report ECOM-5509, AD-767 223 (1973).
48. W. J. Lentz, Generating Bessel functions in Mie scattering calculations using continued fractions, *Appl. Optics* **15,** 668–671 (1976).
49. G. Grehan and G. Gousbet, Mie theory calculations: new progress, with emphasis on particle sizing, *Appl. Optics* **18,** 3489–3493 (1979).
50. A. R. Jones, Calculation of the ratios of complex Riccati–Bessel functions for Mie scattering. *J. Phys. D: Appl. Phys.* **16,** L49–L52 (1983).
51. W. J. Wiscombe, Mie scattering calculations; advances in technique and fast, vector-speed computer codes, Tech. Note NCAR/TN-140+STR. National Center for Atmospheric Research, Boulder, Colorado (1979).
52. W. J. Wiscombe, Improved Mie scattering algorithms, *Appl. Optics* **19,** 1505–1509 (1980).
53. J. D. Felske, Z. Z. Chu and J. C. Ku, Mie scattering subroutines (DBMIE and MIEV0): a comparison of computational times, *Appl. Optics* **22,** 2240–2241 (1983).
54. A. Selamet, Effect of radiation on laminar flame propagation, Ph.D. thesis, University of Michigan, Ann Arbor, Michigan (1989).
55. J. F. Driscoll, D. M. Mann and W. K. McGregor, Submicron particle size measurements in an acetylene–oxygen flame, *Combust. Sci. Technol.* **20,** 41–47 (1979).
56. M. Ben Hamadi, P. Vervisch and A. Coppalle, Radiation properties of soot from premixed flat flame, *Combust. Flame* **68,** 57–67 (1987).
57. E. M. Sparrow and R. D. Cess, *Radiation Heat Transfer*. Hemisphere, Washington, DC, McGraw-Hill, New York (1978).
58. J. D. Felske and C. L. Tien, The use of the Milne–Eddington absorption coefficient for radiative heat transfer in combustion systems, *J. Heat Transfer* **99,** 458–465 (1977).
59. M. Abramowitz and I. A. Stegun, *Handbook of Mathematical Functions* (10th Print), NBS–Applied Mathematics Series 55, pp. 807, 811. U.S. Govt. Printing Office, Washington, DC (1972).
60. W. F. Phillips and V. S. Arpaci, Diatomic gas–thermal radiation interaction: a model equation for the internal fluid, *J. Plasma Physics* **7,** 235–246 (1972).
61. W. F. Phillips and V. S. Arpaci, Monatomic plasma–thermal radiation interaction: a weakly-ionized kinetic model, *J. Plasma Physics* **13,** 523–537 (1975).

EXTENSION SELON PENNDORF DE LA LIMITE DE RAYLEIGH

Résumé—La limite de Rayleigh, dans la théorie de Lorenz–Mie, est étendue par la correction de Penndorf. Pour les facteurs d'efficacité cette extension conduit à $Q^{\mathrm{P}}_{\mathrm{a,s,e}} = Q^{\mathrm{R}}_{\mathrm{a,s,e}}(1+\Pi_{\mathrm{a,s,e}})$ où les indices supérieurs P et R signifient Penndorf et Rayleigh et les indices inférieurs s, a, e respectivement diffusion, absorption, extinction et où Π est la correction de Penndorf à la limite de Rayleigh de $\alpha \cong 0{,}3$ à 0,8, α étant le paramètre de taille des particules. Des contours d'erreur sont générés pour les limites Rayleigh–Penndorf $\alpha = 0{,}3$; 0,5 et 0,7 dans le domaine $1{,}5 \leqslant n \leqslant 2{,}5$ et $0{,}5 \leqslant k \leqslant 1{,}5$ qui couvre celui des propriétés de suies. La signification pratique de la correction de Penndorf est montrée en terme de diagnostiques optiques et de transfert radiatif de chaleur. Les coefficients moyens d'absorption de Planck et de Rosseland basés sur le développement de Penndorf sont liés à ceux basés sur la limite de Rayleigh

$$\kappa^{\mathrm{P}}_{\mathrm{P,R}}/\kappa^{\mathrm{R}}_{\mathrm{P,R}} = 1+\Pi^{\mathrm{P}}_{\mathrm{P,R}}(\underbrace{M_1,\ldots,N_1,\ldots,}_{\text{ondes E.M.}}\ \underbrace{\pi DT/C_2}_{\text{quanta}})$$

où les indices inférieurs P et R signifient les coefficients moyens d'absorption selon Planck et Rosseland, et pour ceux supérieurs P et R Penndorf et Rayleigh, Π la correction de Penndorf dépendant des M et N, fonctions explicites des indices de réfraction et d'absorption des particules et aussi du nombre sans dimension $\pi DT/C_2$ (D étant le diamètre de la particule, T la température et C_2 la seconde constante de rayonnement). Pour des grandes particules et/ou des températures très élevées, le coefficient moyen de Penndorf–Planck s'écarte considérablement du coefficient moyen de Rayleigh–Planck.

RAYLEIGH-GRENZE MIT DER ERWEITERUNG NACH PENNDORF

Zusammenfassung—Die Rayleigh-Grenze der Theorie von Lorenz–Mie wird durch die Penndorf-Korrektur erweitert. Man erhält damit

$$Q^{\mathrm{P}}_{\mathrm{a,s,e}} = Q^{\mathrm{R}}_{\mathrm{a,s,e}}(1+\Pi_{\mathrm{a,s,e}})$$

wobei die Indices P und R für Penndorf und Rayleigh stehen und die Indices s, a und e für Streuung, Absorption und Extinktion. Π ist die Korrektur der Rayleigh-Grenze nach Penndorf. Mit Hilfe dieser Korrektur wird die Rayleigh-Grenze von $\alpha \cong 0{,}3$ auf 0,8 erweitert, wobei α die Partikelgröße darstellt. Fehlerkurven für die Rayleigh- und Penndorf-Grenzen werden für $\alpha = 0{,}3$; 0,5 und 0,7 im Bereich $1{,}5 \leqslant n \leqslant 2{,}5$ und für $0{,}5 \leqslant k \leqslant 1{,}5$ erzeugt, was in etwa den Stoffeigenschaften von Ruß entspricht. Die praktische Bedeutung der Penndorf-Korrektur wird in Bezug auf optische Untersuchungen und Wärmestrahlungsvorgänge gezeigt. Die mittleren Absorptionskoeffizienten nach Planck und Rosseland wurden ebenfalls mit Hilfe der Penndorf-Erweiterung modifiziert. Das Verhältnis zwischen den modifizierten und den Absorptionskoeffizienten aufgrund der Rayleigh-Grenze ergibt sich zu

$$\kappa^{\mathrm{P}}_{\mathrm{P,R}}/\kappa^{\mathrm{R}}_{\mathrm{P,R}} = 1+\Pi^{\mathrm{P}}_{\mathrm{P,R}}(\underbrace{M_1,\ldots,N_1,\ldots,}_{\text{EM-Wellen}}\ \underbrace{\pi DT/C_2}_{\text{Quanten}}).$$

Die tiefgestellten Indices P und R kennzeichnen hier die mittleren Absorptionskoeffizienten nach Planck und Rosseland, die hochgestellten Indices P und R bedeuten wieder Penndorf und Rayleigh. Π ist die Korrektur nach Penndorf. Sie hängt von M und N ab, die explizite Funktionen der Indices von Brechung und Absorption der Teilchen sind, und von der dimensionslosen Kennzahl $\pi DT/C_2$ (D = Partikeldurchmesser, T = Temperatur und C_2 = 2. Strahlungskonstante). Für größere Teilchen und/oder höhere Temperaturen weicht der nach Penndorf bestimmte mittlere Planck'sche Koeffizient stark von dem nach Rayleigh bestimmten ab. Diese Abweichung ist beim nach Penndorf bestimmten Rosseland-Koeffizienten etwas geringer.

РЭЛЕЕВСКИЙ ПРЕДЕЛ–ОБОБЩЕНИЕ ПЕННДОРФА

Аннотация—Рэлеевский предел, используемый в теории Лоренца–Ми, видоизменен с помощью поправки Penndорфа. Для коэффициентов эффективности эта поправка приводит к соотношению вида

$$Q^{\mathrm{P}}_{\mathrm{a,s,e}} = Q^{\mathrm{R}}_{\mathrm{a,s,e}}(1 + \Pi_{\mathrm{a,s,e}})$$

где верхние индексы P и R означают Пенндорф и Рэлей; нижние индексы s, a и e используются соответственно для рассеяния, поглощения и затухания; П означает поправку Пенндорфа к рэлеевскому пределу. Показано, что благодаря этой поправке рэлеевский предел увеличивается с$\alpha \cong 0.3$ до 0.8, где α — параметр, связанный с размером частиц. Контуры ошибок генерируются для пределов Рэлея и Пенндорфа при $\alpha = 0.3$, 0.5 и 0.7 в областях $1.5 \leqslant n \leqslant 2.5$ и $0.5 \leqslant k \leqslant 1.5$, покрывающих диапазон свойств сажи. Практическое значение поправки Пенндорфа демонстрируется с помощью оптической диагностики и лучистого теплопереноса. Кроме того показано, что средние значения коэффициентов поглощения Планка и Росселанда, полученные на основе разложения Пенндорфа, дают значения, которые соотносятся со значениями предела Рэлея как

$$\kappa^{\mathrm{P}}_{\mathrm{P,R}}/\kappa^{\mathrm{R}}_{\mathrm{P,R}} = 1 + \Pi^{\mathrm{P}}_{\mathrm{P,R}}(\underbrace{M_1,\ldots,N_1,\ldots,}_{\text{ЕМ волны}}\ \underbrace{\pi DT/C_2}_{\text{Кванты}})$$

где нижние индексы P и R — средние коэффициенты поглощения Планка и Росселанда, верхние индексы P и R означают Пенндорф и Рэлей, П — поправка Пенндорфа, зависящая от величин M и N, которые являются явными функциями коэффициентов преломления и поглощения частиц и безразмерного числа $\pi DT/C_2$ (D — диаметр частицы, T — температура, C_2 — вторая постоянная излучения). Для частиц большего размера и/или более высоких температур показано, что средний коэффициент Планка с учетом поправки Пенндорфа значительно отклоняется от среднего коэффициента Планка, определяемого по рэлеевскому пределу. Средний коэффициент Росселанда с поправкой Пенндорфа отклоняется меньше.